Cryogenics 60 (2014) 33–43

Contents lists available at ScienceDirect

Cryogenics

journal homepage: www.elsevier.com/locate/cryogenics

First experience with the new Coupling Loss Induced Quench system

E. Ravaioli [a,b,*], V.I. Datskov [a], A.V. Dudarev [a], G. Kirby [a], K.A. Sperin [a,c], H.H.J. ten Kate [a,b], A.P. Verweij [a]

[a] CERN, the European Center for Nuclear Research, POB Geneva 23, 1211 Geneva, Switzerland
[b] University of Twente, Enschede, The Netherlands
[c] University of Birmingham, Birmingham, United Kingdom

ARTICLE INFO

Article history:
Received 18 October 2013
Received in revised form 8 January 2014
Accepted 21 January 2014
Available online 30 January 2014

Keywords:
Accelerator magnet
AC losses
Circuit modeling
Coupling losses
Quench protection
Superconducting coil

ABSTRACT

New-generation high-field superconducting magnets pose a challenge relating to the protection of the coil winding pack in the case of a quench. The high stored energy per unit volume calls for a very efficient quench detection and fast quench propagation in order to avoid damage due to overheating.

A new protection system called Coupling-Loss Induced Quench (CLIQ) was recently developed and tested at CERN. This method provokes a fast change in the magnet transport current by means of a capacitive discharge. The resulting change in the local magnetic field induces inter-filament and inter-strand coupling losses which heat up the superconductor and eventually initiate a quench in a large fraction of the coil winding pack.

The method is extensively tested on a Nb–Ti single-wire test solenoid magnet in the CERN Cryogenic Laboratory in order to assess its performance, optimize its operating parameters, and study new electrical configurations. Each parameter is thoroughly analyzed and its impact on the quench efficiency highlighted.

Furthermore, an alternative method is also considered, based on a CLIQ discharge through a resistive coil magnetically coupled with the solenoid but external to it. Due to the strong coupling between the external coil and the magnet, the oscillating current in the external coil changes the magnetic field in the solenoid strands and thus generates coupling losses in the strands. Although for a given charging voltage this configuration usually yields poorer quench performance than a standard CLIQ discharge, it has the advantage of being electrically insulated from the solenoid coil, and thus it can work with much higher voltage.

1. Introduction

New-generation high-field superconducting magnets require a very efficient quench protection system which can quickly discharge the energy stored in a coil. Conventional protection systems, such as energy-extraction systems and quench heaters, have drawbacks and limitations. The value of an extraction resistor R_{EE}, and hence the decay time, is limited by the maximum safe voltage in the circuit $U_{EE} = R_{EE} \cdot I$. Quench heaters rely on the thermal diffusion across insulation layers, an inherently slow process, and increase the risk of electrical break-down.

A new Coupling-Loss Induced Quench (CLIQ) protection system was recently developed at CERN. This method features a capacitive discharge through a current lead connected to an internal point of a coil, resulting in a fast change of the local magnetic field in the conductor. As a result, coupling losses are generated in the copper matrix of the superconductor which heat up the coil and quickly initiate a quench due to the enhanced temperature. The CLIQ was successfully tested on a 2 m long quadrupole magnet in the CERN magnet test facility [1–2].

Nevertheless, testing the method on a small-scale test magnet allows a more thorough analysis of the system behavior thanks to the reduced time required for each test and to the additional voltage taps available for measurements. The CLIQ is tested on a Nb–Ti solenoid magnet at CERN in order to assess its performance, optimize its operating parameters, and study various electrical configurations. The effect of each parameter on the system performance is thoroughly investigated.

Moreover, an alternative CLIQ design is tested, based on a capacitive discharge through a copper external coil surrounding the solenoid magnet. Such a system is electrically insulated from the magnet but can deposit heat in the solenoid coil by introducing coupling losses in its strands.

2. The Coupling Loss Induced Quench system

The CLIQ system, presented in [1–2], is schematized in Fig. 1. Its design is based on a protection scheme proposed in [3–4] but with the addition of the patented reverse diode D [5]. The CLIQ is

* Corresponding author at: CERN, Switzerland.
E-mail address: emmanuele.ravaioli@cern.ch (E. Ravaioli).

http://dx.doi.org/10.1016/j.cryogenics.2014.01.008
0011-2275/

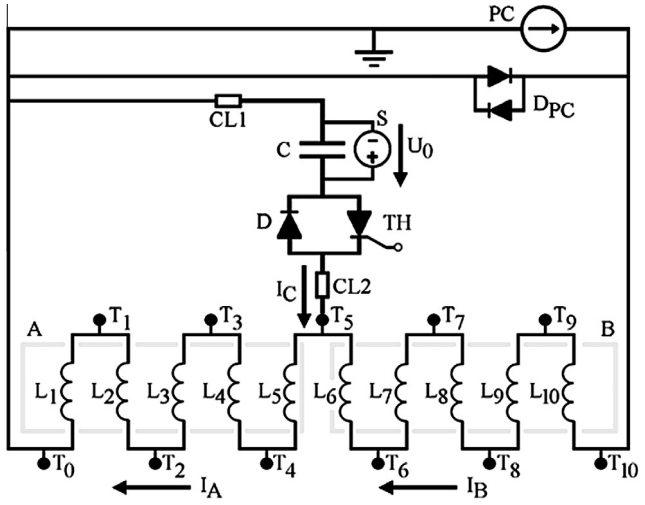

Fig. 1. Schematic of the Coupling-Loss Induced Quench (CLIQ) protection system and of the test solenoid magnet (Configuration T0–T5, see Section 3).

composed of a capacitor bank C, a floating voltage supply S, two additional resistive current leads CL1 and CL2 connecting the system to the superconducting coil, a thyristor TH, and a reverse diode D. The capacitor bank is charged by S with a voltage U_0. When a quench is detected, the thyristor is activated resulting in a current I_C to be discharged through CL1 and CL2. This introduces a current change with opposite direction in the two branches of the coil A and B. The presence of the reverse diode allows continuous oscillations of I_C.

The time evolution of the CLIQ system is found by solving the following equivalent system:

$$\begin{cases} I_A = I_C + I_B \\ (L_A + M_{AB}) \cdot \dot{I}_A + (L_B + M_{AB}) \cdot \dot{I}_B + R_{Q,A} \cdot I_A + R_{Q,B} \cdot I_B + U_D = 0 \\ U_C = L_A \cdot \dot{I}_A + M_{AB} \cdot \dot{I}_B + R_{Q,A} \cdot I_A + (R_{CL1} + R_{CL2}) \cdot I_C + U_{TH} \\ I_C = C \cdot \dot{U}_C \\ I_A(0) = I_B(0) = I_0 \\ I_C(0) = \dot{U}_C(0) = 0 \\ U_C(0) = U_0, \end{cases} \tag{1}$$

where I_A and I_B are the current flowing in A and B, L_A and L_B the self-inductances of A and B, M_{AB} their mutual inductance, $R_{Q,A}$ and $R_{Q,B}$ the quench resistance developed in A and B, U_D the voltage drop across the diode D_{PC}, U_C the voltage across C, R_{CL1} and R_{CL2} the resistance of CL1 and CL2, U_{TH} the voltage drop across the thyristor TH, and I_0 the initial magnet transport current.

At the moment of the CLIQ discharge, it can be assumed that the large majority of the coil is in superconducting state, i.e. $R_{Q,A} \approx R_{Q,B} \approx 0$. Under this assumption, the system can be analyzed as a series RLC circuit composed of the equivalent circuit resistance $R_{eq} = R_{CL1} + R_{CL2} + U_{TH}/I_C$, the equivalent inductance of the coil circuit L_{eq}, and the discharging capacitance C. L_{eq} can be calculated by solving system (1) for constant L_A, L_B, and M_{AB}:

$$L_{eq} = (L_A \cdot L_B - M_{AB}^2)/(L_A + L_B + 2M_{AB}), \tag{2}$$

which correspond to the impedance of two mutually coupled inductors in parallel. In real cases the self-inductances L_A and L_B decrease with the frequency due to dynamic effects linked to coupling currents, which change the amount of magnetic flux linked to the superconducting coil. It can be shown that if $R_{eq} < 2\sqrt{L_{eq}/C}$ the response of the RLC system is a damped oscillation. Neglecting the limited voltage drop across D_{PC}, the voltage across C and the current I_C are equal to:

$$U_C(t) = U_0 \cdot \exp(-\alpha t) \cdot \left[\cos(\omega t) + \frac{\alpha}{\omega} \sin(\omega t)\right], \tag{3}$$

and

$$I_C(t) = C\frac{dU_C(t)}{dt} = -CU_0 \cdot \frac{\omega^2 + \alpha^2}{\omega} \cdot \exp(-\alpha t) \cdot \sin(\omega t), \tag{4}$$

with $\omega = \sqrt{\omega_0^2 - \alpha^2}$, $\omega_0 = 1/\sqrt{L_{eq} \cdot C}$, and $\alpha = R_{eq}/(2L_{eq})$. In most practical cases $\alpha \ll \omega_0$ and thus $\omega \approx \omega_0$. Assuming an initial transport current I_0, the current in the two branches is:

$$I_A(t) = I_0 + (L_B + M_{AB})/(L_A + L_B + M_{AB}) \cdot I_C = I_0 + f_{g,A} \cdot I_C, \tag{5a}$$

and

$$I_B(t) = I_0 - (L_A + M_{AB})/(L_A + L_B + M_{AB}) \cdot I_C = I_0 - f_{g,B} \cdot I_C, \tag{5b}$$

where $f_{g,A}$ and $f_{g,B}$ are purely geometric parameters if the self and mutual inductances are constant. The introduced current change in the two branches is thus

$$\begin{aligned} dI_A/dt &= f_{g,A} \cdot dI_C/dt \\ &= CU_0 \cdot \frac{\omega^2 + \alpha^2}{\omega} \cdot f_{g,A} \cdot [\omega \cdot \exp(-\alpha t) \cdot \cos(\omega t) - \alpha \\ &\quad \cdot \exp(-\alpha t) \cdot \sin(\omega t)], \end{aligned} \tag{6a}$$

and

$$\begin{aligned} dI_B/dt &= f_{g,B} \cdot dI_C/dt \\ &= -CU_0 \cdot \frac{\omega^2 + \alpha^2}{\omega} \cdot f_{g,B} \cdot [\omega \cdot \exp(-\alpha t) \cdot \cos(\omega t) - \alpha \\ &\quad \cdot \exp(-\alpha t) \cdot \sin(\omega t)]. \end{aligned} \tag{6b}$$

These oscillating currents change the local magnetic field inside the coil. Let z and r be the two directions perpendicular to the transport-current direction. In the case of a solenoid magnet, z is parallel to the solenoid axis and r is parallel to its radius. In steady-state the magnetic field along z and r in each superconducting strand k is a linear function of the transport currents in A and B, hence

$$B_{az,k} = f_{z,A,k} I_A + f_{z,B,k} I_B, \tag{7a}$$

and

$$B_{ar,k} = f_{r,A,k} I_A + f_{r,B,k} I_B. \tag{7b}$$

The parameters appearing in Eqs. (7a) and (7b) can be calculated by means of dedicated software, such as [6]. However, in a solenoid magnet usually $B_{ar} \ll B_{az}$. Hence, let the steady-state magnetic field in the z direction be $B_{a,k} = f_{A,k} \cdot I_A + f_{B,k} \cdot I_B$. When a superconducting strand is subjected to an applied field change $dB_{a,k}/dt$, an induced field change $dB_{i,k}/dt$ is created in the opposite direction due to inter-filament coupling currents [7]. Thus, the total local magnetic-field change is:

$$\begin{aligned} \frac{dB_{t,k}}{dt} &= \frac{dB_{a,k}}{dt} + \frac{dB_{i,k}}{dt} \\ &= CU_0 \cdot \frac{\omega^2 + \alpha^2}{\omega} \cdot (f_{A,k} \cdot f_{g,A} - f_{B,k} \cdot f_{g,B}) \cdot [\omega \cdot \exp(-\alpha t) \\ &\quad \cdot \cos(\omega t) - \alpha \cdot \exp(-\alpha t) \cdot \sin(\omega t)] \\ &\quad \cdot \left[1 - \exp\left(-\frac{t}{\tau_{if,k}}\right)\right], \end{aligned} \tag{8}$$

with $\tau_{if,k}$ the characteristic time constant of the inter-filament coupling currents,

$$\tau_{if,k} = \frac{\mu_0}{2\rho_{eff,k}} \left(\frac{l_f}{2\pi}\right)^2 = \beta_k \frac{\mu_0}{2}, \tag{9}$$

with l_f the filament twist-pitch, ρ_{eff} the effective transverse resistivity of the matrix, $\mu_0 = 4\pi \times 10^{-7}$ T m/A the magnetic permeability of

vacuum, and $\beta_k = (l_f/2\pi)^2/\rho_{eff,k}$. The inter-filament coupling losses per unit volume induced in a cable by the oscillating current are [7]

$$P_{if,k} = \left(\frac{l_f}{2\pi}\right)^2 \frac{1}{\rho_{eff,k}} \left(\frac{dB_{t,k}}{dt}\right)^2 = \beta_k \left(\frac{dB_{t,k}}{dt}\right)^2 = \frac{2}{\mu_0}\tau_{if,k}\left(\frac{dB_{t,k}}{dt}\right)^2. \quad (10)$$

If a strand is subjected to a magnetic-field change both in the z and r direction, their effects superpose and inter-filament coupling losses generated in both directions can be similarly calculated. Furthermore, if the coil is composed of a multi-strand conductor, similar coupling currents are induced between the cable strands. In the case of a Rutherford-type cable the amplitude and time constant of these inter-strand coupling currents are given in [7].

The total energy per unit volume deposited in the coil after a CLIQ discharge can be calculated by integrating in time Eq. (10). By combining Eqs. (8) and (10) this integral for a strand k reads.

$$\begin{aligned}\int P_{if,k}dt &= \int \frac{2}{\mu_0}\tau_{if,k}\left(\frac{dB_{t,k}}{dt}\right)^2 dt \\ &= \frac{2}{\mu_0}\cdot\left[CU_0\cdot\frac{\omega^2+\alpha^2}{\omega}\cdot(f_{A,k}\cdot f_{g,A} - f_{B,k}\cdot f_{g,B})\right]^2\cdot \\ &\int \tau_{if,k}\cdot\{[\omega\cdot\exp(-\alpha t)\cdot\cos(\omega t) - \alpha\cdot\exp(-\alpha t)\cdot\sin(\omega t)]\cdot \\ &\times\left[1-\exp\left(-\frac{t}{\tau_{if,k}}\right)\right]\Big\}^2 dt. \end{aligned} \quad (11)$$

The integral is numerically solved for various operating parameters in order to assess their impact on the system performance. The results of these calculations are presented in the following section together with a selection of test results.

Once the oscillations introduced by CLIQ are completely damped, $I_C \approx 0$ and thus the system (1) can be reduced to

$$\begin{cases} I_A \approx I_B \\ (L_A + L_B + 2M_{AB})\cdot\dot{I}_A + (R_{Q,A} + R_{Q,B})\cdot I_A + U_D = 0 \end{cases}. \quad (12)$$

During this transient, the magnet current is discharged following the relation:

$$dI_A/dt = -I_A/\tau_d, \quad (13)$$

where the time constant $\tau_d = (L_A + L_B + 2\,M_{AB})/(R_{Q,A} + R_{Q,B})$ generally decreases during the discharge due to the increase of the quench resistance.

3. Quench protection using the CLIQ

The CLIQ system is tested on a Nb–Ti single-wire solenoid magnet in the CERN Cryogenic Laboratory in order to assess its performance and investigate different electrical configurations.

3.1. Test solenoid magnet

Fig. 1 shows the test circuit. By-pass diodes D_{PC} are installed across the power converter to protect it during the CLIQ discharge. The main parameters of the magnet, originally a prototype for the AEGIS experiment [8], are summarized in Table 1 [9]. It is composed of ten concentric layers powered in series; CL1 and CL2 can be connected to dedicated taps located between every two layers (see T1–T9 in Fig. 1), or to one of the two main current leads of the power converter (T0 and T10). Each configuration is denominated following the taps to which CL1 and CL2 are connected; as an example, Fig. 1 shows Configuration T0–T5 where the positive and negative terminals of CLIQ are connected to taps T0 and T5, respectively.

The CLIQ capacitor bank is composed of 8 film capacitors with capacitance of 1.1 mF and rated for ±1.1 kV. The capacitors are connected in parallel; thus, by removing some of them the total capacitance of the bank C can be varied between 1.1 and 8.8 mF. The maximum charging voltage U_0 used during the tests is 250 V, safely below the maximum turn-to-turn voltage (~1 kV) and voltage to ground (~5 kV) that the insulation of the magnet wire can sustain.

Furthermore, a copper bandage coil is wrapped around the solenoid. This resistive coil, originally designed as a mechanical reinforcement to the magnet coil, is used as a mean to measure the inductive component of the voltage across the solenoid. In fact, the voltage over the bandage coil is proportional to the inductive voltage over the magnet, $U_{\text{band}} = f_{A,\text{band}}\cdot dI_A/dt + f_{B,\text{band}}\cdot dI_B/dt$. This external coil is composed of two layers of wire with the same number of turns and cross-section of the superconducting coil composing the magnet.

Table 1
Main parameters of the test solenoid magnet.

Parameter	Value
Nominal current, I	400 A
Central magnetic field at I = 400 A	2.5 T
Peak magnetic field in the coil at I = 400 A	2.9 T
Coil critical current at 3.8 T, 4.2 K	521 A
Operating temperature	4.2 K
Self-inductance of magnet coil	462 mH
Magnet coil length	199 mm
Magnet inner diameter	237 mm
Magnet outer diameter	256.6 mm
Number of layers of magnet coil	10
Turns per layer	157
Conductor width	0.8 mm
Conductor height	1.25 mm
Cu/Nb–Ti ratio	4.2
RRR	91
Self-inductance of bandage coil	20.6 mH
Mutual inductance between magnet and bandage coil	93.0 mH
Bandage coil length	199 mm
Bandage coil inner diameter	257 mm
Bandage coil outer diameter	261 mm
Number of layers of bandage coil	2

3.2. Effect of the coupling losses on the dynamic inductance of the solenoid magnet

When the magnet is in the superconducting state its dynamic inductance is significantly decreased due to the presence of coupling losses which reduce the magnetic flux coupled to the superconducting coil. As an example, Configuration T0–T6 is considered with L_A = 163 mH, L_B = 78 mH, and M_{AB} = 109 mH; thus, following (2) L_{eq} = 2.1 mH. Discharging a capacitor C = 4.4 mF charged with U_0 = 100 V, following (4) the system oscillates at $f_0 = \omega/(2\pi) \approx 50$ Hz. This frequency is indeed measured when discharging the CLIQ system at I_0 = 0 when the coil is at cryogenic temperature ($T \sim 10$ K) but not in the superconducting state, see Fig. 2. However, when the coil is in superconducting state ($T \sim 4$ K) the system oscillates at $f_{SC} \approx 77$ Hz, 50% larger than f_0. This result shows that at this frequency L_{eq} in superconducting state is about 40% of the value calculated using (2) for frequency-independent L_A, L_B, and M_{AB}. The comparison between I_C measured in normal and superconducting state is shown in Fig. 2.

3.3. Coupling-Loss Induced Quench

Fig. 3 shows the evolution in time of the currents I_A and I_B after triggering the CLIQ at I_0 = 300 A. The fast current change introduces enough coupling losses to initiate a quench in the solenoid, and the developing quench resistance forces the discharge of the transport current. The effective coil resistance, also shown in Fig. 3, is deduced by subtracting the inductive voltage over the magnet coil,

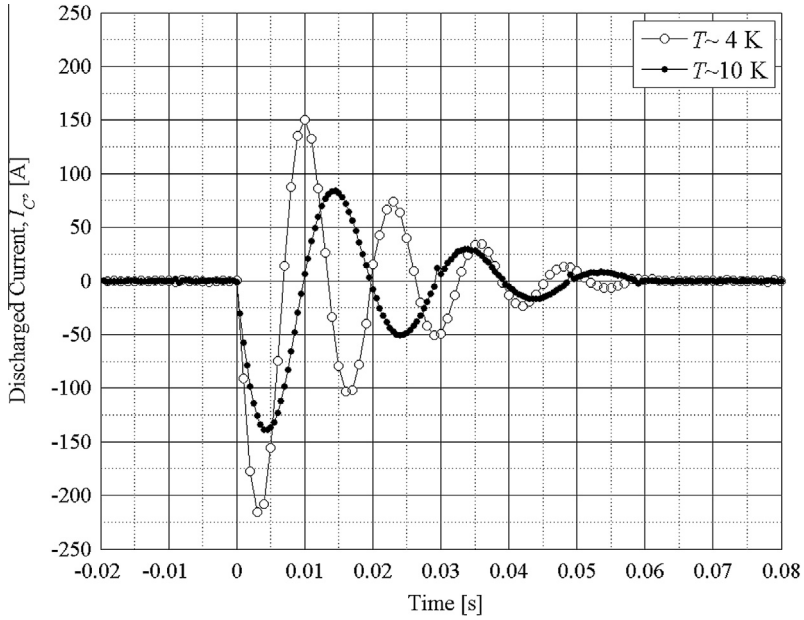

Fig. 2. CLIQ discharges at $I_0 = 0$ (Configuration T0–T6, $U_0 = 100$ V, $C = 4.4$ mF). Measured currents I_C versus time with the coil in normal and in superconducting state.

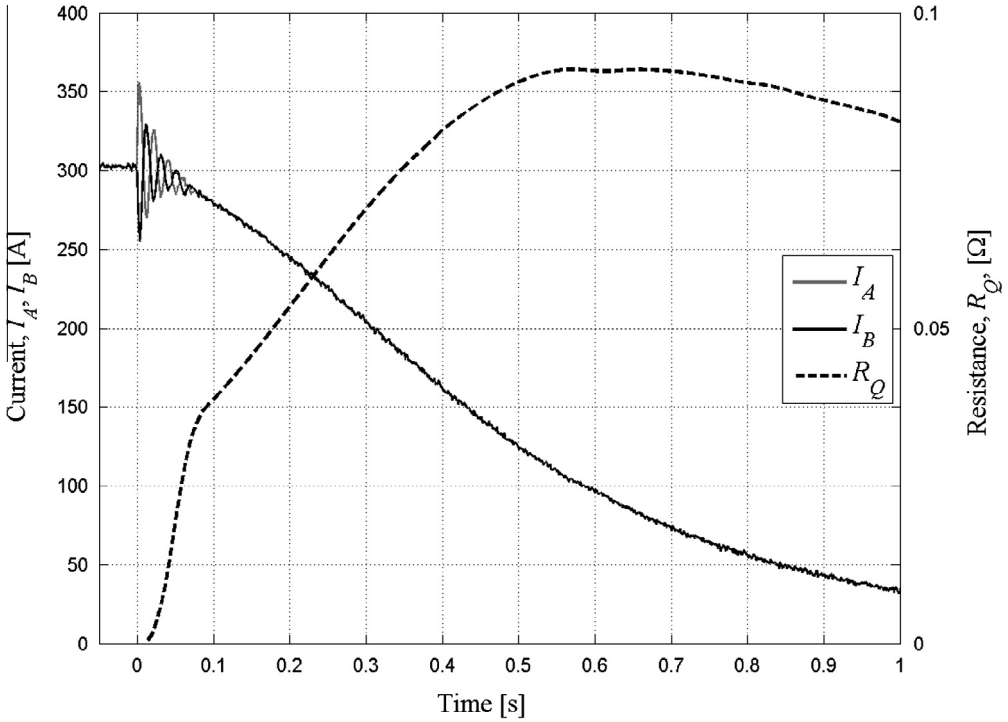

Fig. 3. Measured currents I_A and I_B versus time and calculated effective coil resistance R_Q versus time after a CLIQ discharge at $I_0 = 300$ A (Configuration T0-T5, $U_0 = 75$ V, $C = 4.4$ mF).

which is proportional to the voltage over the bandage coil, from the total voltage across the magnet,

$$R_Q = (U_{tot} - U_{ind})/I_A = (U_{tot} - f_{band}U_{band})/I_A. \quad (14)$$

The value of $f_{band} \approx 5$ can be calculated with dedicated software [6] or simply deduced as the ratio U_{ind}/U_{band} measured during a transient with constant ramp-rate. This equation is not valid during the first tens of milliseconds after a CLIQ discharge because $I_A \neq I_B$. Nevertheless, observing the behavior of R_Q provides useful information about the thermal dynamic of the system and about the effectiveness of the CLIQ system in quenching the coil. Three distinct phases are visible in the evolution of R_Q. After the CLIQ triggering a sharp increase is observed while the coil turns from normal to resistive state. After about 75 ms the whole coil is quenched, and $R_Q \approx 350$ mΩ, roughly corresponding to the resistance of the coil just above the critical temperature. The subsequent rise of R_Q is due to the increase in the coil temperature through Ohmic losses. Finally, R_Q goes down because the temperature in the coil decreases due to the helium cooling.

Furthermore, the voltage across each layer l is measured and used to calculate the effective quench resistance developed in each layer by similarly subtracting the inductive component,

$$R_l = (U_l - U_{\mathrm{ind},l})/I_l = (U_l - f_{\mathrm{band},l}U_{\mathrm{band}})/I_l. \quad (15)$$

The linear factors of proportionality $f_{\mathrm{band},l}$ can be calculated [6] or defined as the ratio U_l/U_{band} measured during a transient with steady ramp-rate. During the first tens of milliseconds following the CLIQ triggering the dynamic effects are relatively strong and the use of these constant parameters may lead to significant errors in the calculation of R_l. However, calculating R_l is an effective means to assess which layers are the first to quench and how fast the quench propagation is.

Fig. 4 shows the layer-by-layer quench resistance during a CLIQ discharge. Layers L8, L9, and L10 are more difficult to quench because the local magnetic field is lower and hence the current-sharing temperature is higher. Furthermore, the resistance of layers L1 and L10 starts decreasing sooner than the other layers as they are nearest to the helium bath. The middle layers quench first and take longer to recover as less heat is extracted by the helium cooling.

4. Optimizing the CLIQ performance

About one thousand CLIQ tests have been performed on the test solenoid magnet in order to study its efficiency under different operating conditions, investigate the effect of various system parameters, and optimize its performance. The key parameters under study are the initial current I_0, the charging voltage U_0, the capacitance C, the inter-filament coupling loss time-constant τ_{if}, and the position of the injection/extraction points.

4.1. Effect of I_0

In the first approximation the current I_C discharged by the CLIQ and the impedance of the two branches A and B do not depend on the initial current I_0 flowing in the solenoid. In fact, the only terms dependent on I_0 in the equations of system (1) are those related to the quench resistance which can be neglected before the CLIQ discharge ($R_{Q,A} \approx R_{Q,B} \approx 0$). Therefore, the current change in the coil, and thus the introduced coupling losses, are independent of I_0. Nevertheless, the energy required to quench the coil reduces with increasing current, because the current-sharing temperature is lower. Fig. 5 shows the measured I_A after triggering a 4.7 mF, 150 V CLIQ at various current levels. It can be seen that – as expected – the AC component of the current is almost independent of I_0, but at higher current the solenoid is discharged more quickly because the coil resistance increases faster. This is clearly shown in Fig. 6 for the same set of transport currents. For higher I_0 the fraction of coil quenched by the CLIQ increases, and the Ohmic losses developed in the coil, proportional to the fraction of quenched coil and to the square of the transport current, cause a faster rise of the coil resistance. Below a certain current, the Ohmic losses in the coil become smaller than the heat removed by the helium surrounding the solenoid, and thus the coil temperature goes down, and hence R_Q is decreased. In the case of $I_0 = 100$ A, the coil reaches an equilibrium state between Ohmic loss and helium cooling, and the coil resistance remains almost constant throughout the current discharge.

4.2. Effect of U_0

The impact of U_0 on the total energy deposited with a CLIQ discharge can be easily evaluated by considering a simplified case where the magnetic field in any point of the magnet is purely parallel to the coil axis ($B_{ar,k} = 0$) and the resistance in the discharge circuit is zero, i.e. $R_{eq} = \alpha = 0$. Under such assumptions, Eq. (11) is reduced to

$$\int P_{if,k}dt \approx \frac{2}{\mu_0}\cdot\frac{U_0^2}{L_{eq}^2}\cdot(f_{A,k}\cdot f_{g,A} - f_{B,k}\cdot f_{g,B})^2\cdot\int \tau_{if,k} \cdot\left\{\cos(\omega t)\cdot\left[1-\exp\left(-\frac{t}{\tau_{if,k}}\right)\right]\right\}^2 dt. \quad (16)$$

Thus, P_{if} in any strand of the magnet can be maximized by increasing the charging voltage U_0 to the maximum voltage allowed in the circuit. The deposited coupling loss has a direct effect on the quench efficiency, as shown in Fig. 7 where the time required to quench 90% of the coil is plotted for varying I_0 and U_0. These values are deduced as the time when the calculated R_Q is larger than 90% of the coil resistance at cryogenic temperature ($T \sim 10$ K); since the temperature in most of the coil does not raise much during the short considered transients, this approximation seems acceptable.

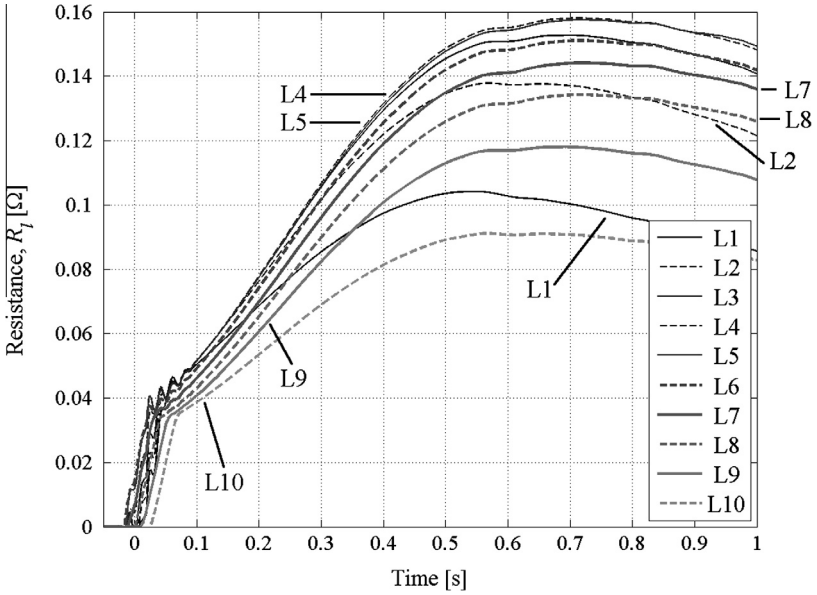

Fig. 4. Calculated effective quench resistance in each layer R_l versus time after a CLIQ discharge at $I_0 = 300$ A (Configuration T0–T5, $U_0 = 75$ V, $C = 4.4$ mF).

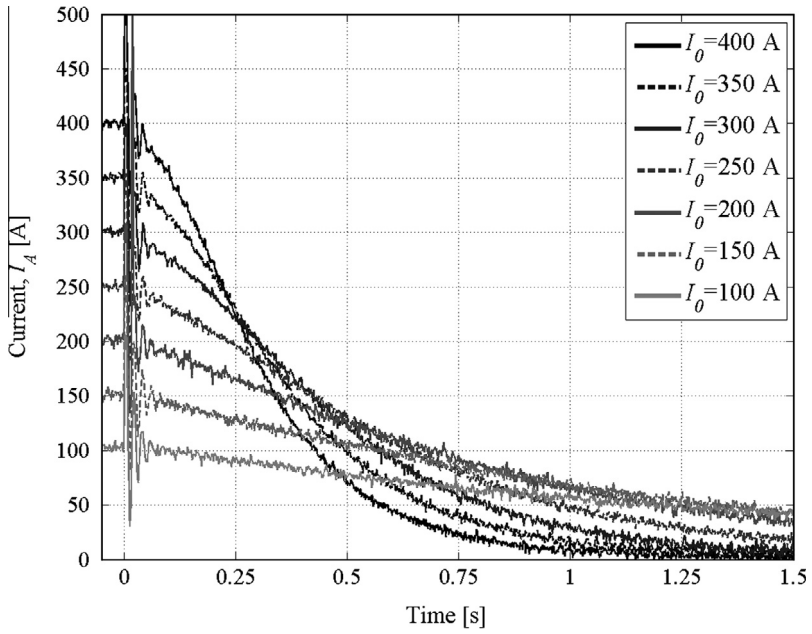

Fig. 5. Measured current I_A versus time during a CLIQ discharge at various initial currents I_0 (Configuration T6–T0, C = 4.7 mF, U_0 = 150 V).

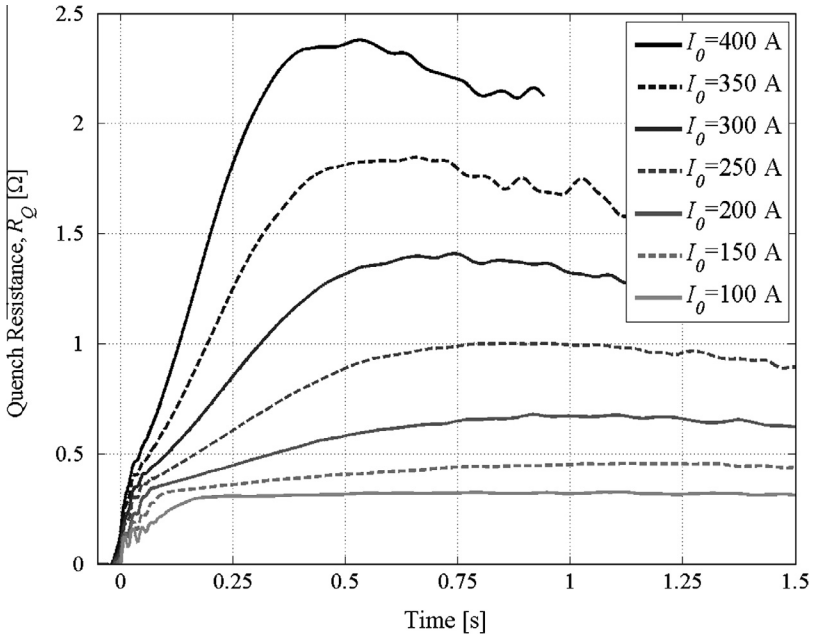

Fig. 6. Calculated effective coil resistance R_Q versus time after a CLIQ discharge at various initial currents I_0 (Configuration T6–T0, C = 4.7 mF, U_0 = 150 V).

4.3. Effect of C and τ_{if}

Eqs. (10) and (11) show that the dependency of the inter-filament coupling loss P_{if} on their time constant τ_{if} is twofold. In fact, on the one hand P_{if} is linearly proportional to τ_{if}, but on the other hand it depends on $1-\exp(-t/\tau_{if})$. As a result, for larger τ_{if} the amplitude of the coupling losses increases, but they also need more time to develop.

For this reason, if the period of the CLIQ oscillations is too short, i.e. $1/f \ll \tau_{if}$, the coupling losses do not have enough time to fully develop and the heat deposited by a CLIQ discharge is limited. This result can be observed in Fig. 8, where the coupling losses per unit volume deposited in the first 50 ms after a CLIQ discharge, calculated by numerically solving the integral in Eq. (11), are shown for varying $1/f$ and τ_{if}. As expected very little loss is introduced by CLIQ if $1/f \ll \tau_{if}$. Similarly, it can be noted that for very small values of τ_{if} the CLIQ introduces limited coupling losses due to the linear dependency of the deposited losses on the value of τ_{if}.

Thus, for any oscillation period an optimum value of τ_{if} exists that maximizes the coupling losses introduced by a CLIQ discharge. As shown in Eq. (9), the value of τ_{if} depends on the filament twist-pitch and on the effective resistivity of the matrix.

Finally, one can observe that increasing the oscillation period, proportional to $\sqrt{C}$, monotonically enhances the deposited coupling loss. This result is confirmed by the analysis of the coil quench resistance obtained after a CLIQ discharge. Fig. 9 shows a comparison between the calculated R_Q developed after triggering a T0–T5, 75 V CLIQ system at I_0 = 200 A for various values of C. As

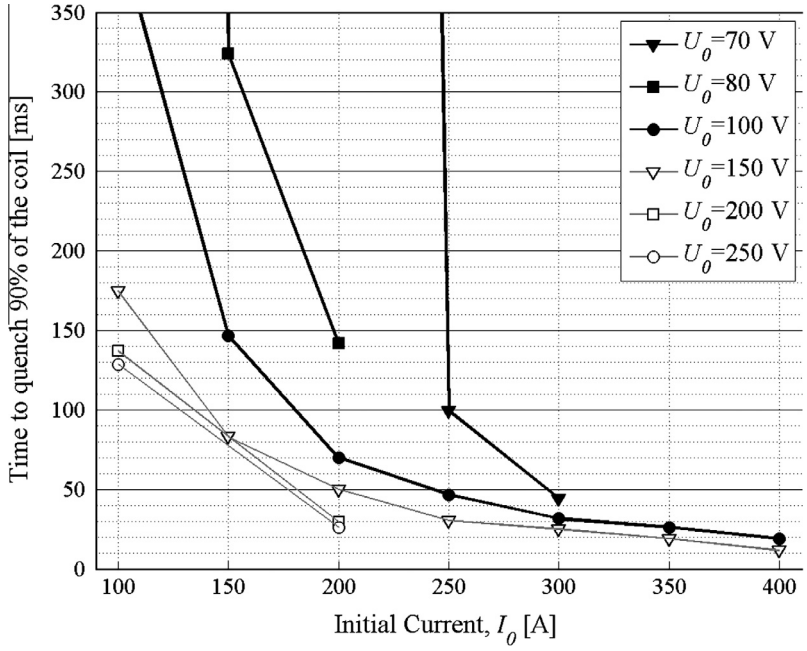

Fig. 7. Calculated time required to quench 90% of the coil after a CLIQ discharge versus I_0, for various charging voltages U_0 (Configuration T6–T0, C = 4.7 mF).

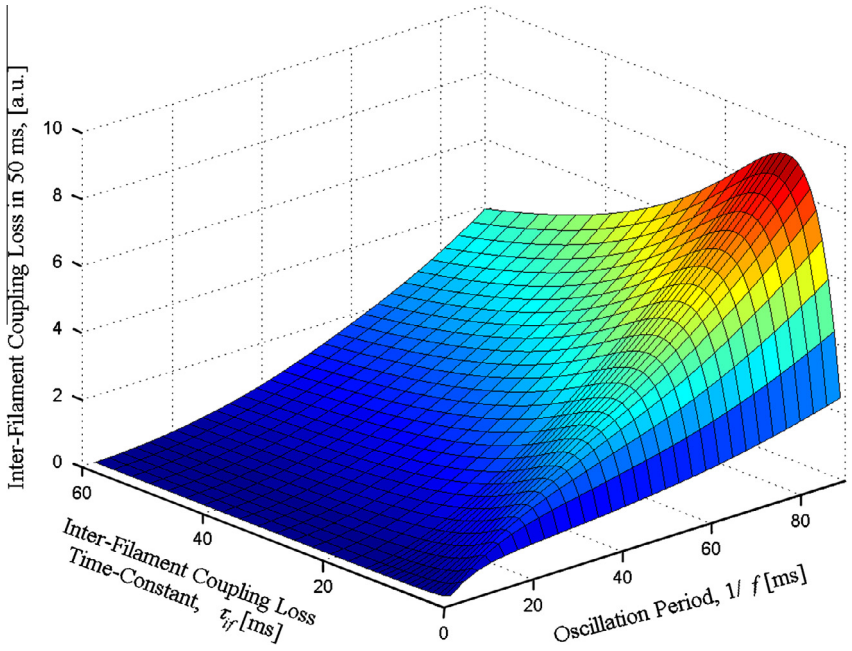

Fig. 8. Calculated inter-filament coupling loss per unit volume introduced during the first 50 ms after a CLIQ discharge, normalized to the energy required to quench a unit volume, versus the oscillation period 1/f and the inter-filament coupling loss time-constant τ_{if} (Configuration T0–T5, L_{eq} = 2.3 mH, U_0 = 75 V, I_0 = 200 A, f_k = 3.7 mT/A, R_{eq} = 250 mΩ).

expected, the quench performance improves with larger capacitance. In these operating conditions, a value of C = 2.2 mF is not sufficient to initiate a quench in the solenoid, whereas increasing C up to 8.8 mF, thus doubling the oscillation period, quenches the whole coil in less than 100 ms.

4.4. Effect of the positioning of CLIQ injection/extraction points

The positioning of the CLIQ injection and extraction connections to the solenoid magnet (CL1 and CL2, see Fig. 1) greatly affects the system behavior and performance. Firstly, the oscillation frequency f of the RLC discharge system can be increased by placing the internal current lead (see CL2 in Fig. 1) closer to one side of the coil, thus reducing L_A or L_B and hence L_{eq}. Enhancing f increases the current change rate, and thus the coupling loss, in the branch of the coil with smaller impedance; however, less symmetric configurations also produce inhomogeneous heat deposition in the coil due to the different current change in the branches A and B. Secondly, discharging an AC current through an internal current lead placed between two layers of a solenoid effectively splits the coil in two

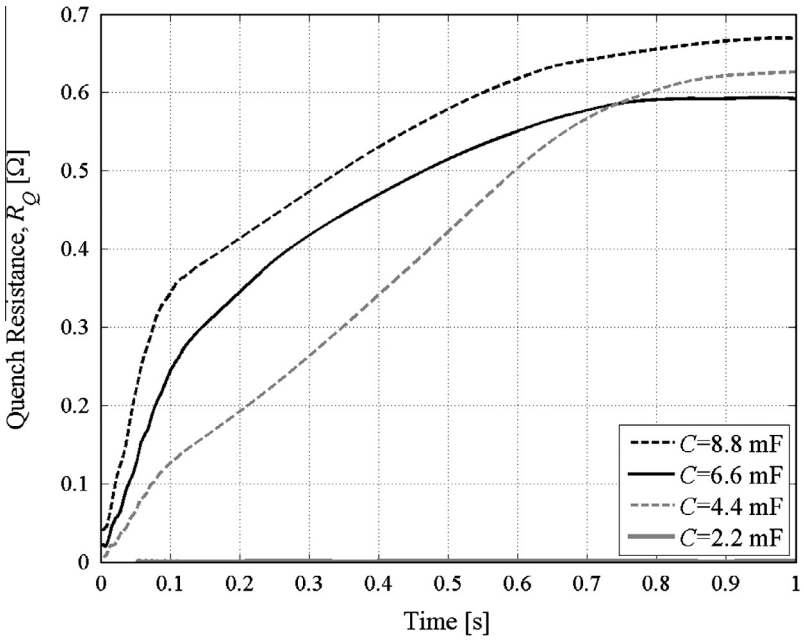

Fig. 9. Calculated effective coil resistance R_Q versus time after a CLIQ discharge at various capacitances C (Configuration T0–T5, I_0 = 200 A, and U_0 = 75 V).

solenoids subjected to opposite current change. As a result, the two layers adjacent to CL2, located at the boundary between the two coil branches, undergo the maximum magnetic-field change.

This result is evident when observing Fig. 10, where the time required to quench each of the ten layers of the solenoid is plotted for a range of electrical configurations featuring a 75 V, 8.8 mF CLIQ discharge between a side of the magnet (T0) and various points in the middle of the coil (from T1 to T9). As expected, the first layers to quench are those adjacent to the CLIQ injection points. Furthermore, it can be seen that the layers located in the inner region of the solenoid are easier to quench due to the higher magnetic field and hence smaller temperature margin. On the contrary, Configuration T9–T0, not shown in the plot, deposits most of the heat in the two outermost layers (L9 and L10) which are the most difficult to quench. As a result, no quench is initiated in the coil before several hundred milliseconds.

In all the other shown configurations, once a quench is initiated the Ohmic heat generated in the portion of coil already in normal state diffuses to adjacent layers and thus the quench propagates. At this current of I_0 = 200 A, 10–20 ms are needed in order to fully propagate the quench to a neighboring layer. However, one can observe that the heat propagation is slower in the outer, low magnetic-field region of the solenoid. For this reason Configuration T1–T0, which initiates a quench in L1 and L2, requires the longest

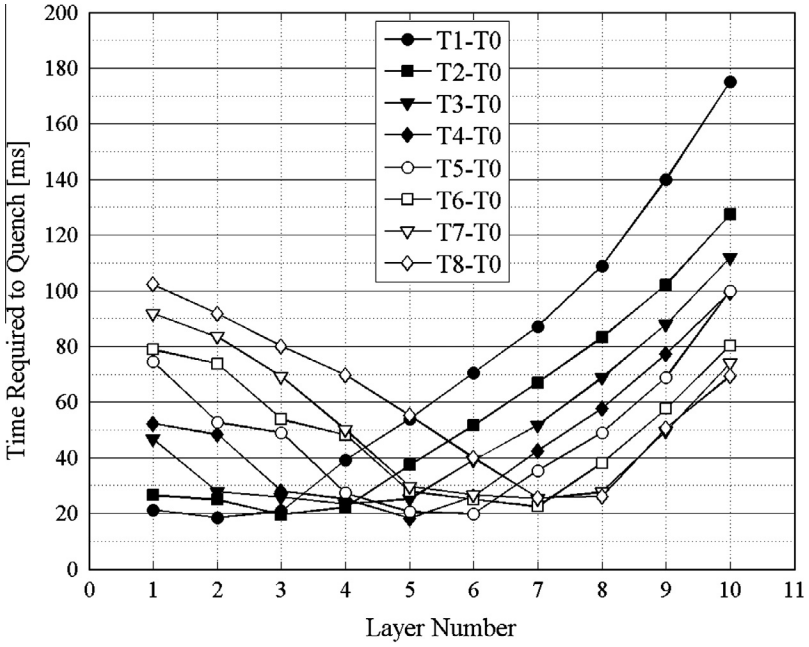

Fig. 10. Calculated time required to quench 90% of each of the ten layers of the solenoid magnet after a CLIQ discharge for various configurations (T1-T0· · ·T8-T0, I_0 = 200 A, U_0 = 75 V, and C = 8.8 mF).

time to quench the whole coil because the heat needs to propagate through the layers with the highest margin to quench. As a contrast, Configurations T5–T0 and T6–T0 are particularly effective in quenching the whole coil, because a quench is initiated right at the center of the solenoid and the Ohmic heat can therefore propagate in both directions toward inner and outer layers. Moreover, these more symmetric configurations reduce the mechanical stress on the peripheral layers.

A further improvement in the CLIQ performance can be achieved by creating two separate zones where a quench is initiated due to high coupling loss. This can be obtained by connecting both CLIQ terminals CL1 and CL2 to injection/extraction points in the interior of the magnet coil (T1–T9), thus introducing a large magnetic-field change in two separate regions of the solenoid. The equivalent inductance of the discharge system can still be calculated using Eq. (2), where L_A and L_B are the self-inductance of the layers between and outside the two extraction points, respectively. In fact, the two ends of the solenoid coil are connected through two diodes in antiparallel configuration, and in the first approximation the two portions of the magnet outside the extraction points can be considered electrically in series.

An optimum positioning of CL1 and CL2 allows depositing heat in two well-distributed zones thus maximizing the quench propagation. Fig. 11 shows the quench performance of two configurations designed following this principle, T8–T3 and T6–T4, as compared to two configurations presented before, T0–T2 and T5–T0. It can be observed that the CLIQ configurations discharging through two internal current leads effectively create two distinct quench zones and are quicker to turn to normal state the whole winding pack. Configuration T8–T3 starts the quench in layers L3 and L8, whereas Configuration T6–T4 in L4 and L7.

A top-efficiency CLIQ system for the protection of solenoid magnets could include multiple CLIQ's discharging an AC current with opposite polarity in every other layer, thus simultaneously generating high coupling losses in all the layers of the coil and generate a very homogeneous quench initiation. The size and cost of one CLIQ system are similar to those of a conventional quench-heater based protection system, and thus the installation of multiple CLIQ's seems a viable solution for protecting a superconducting solenoid magnet. The components of CLIQ are robust and easy to replace in case of damage. Furthermore, one or more CLIQ's can be used to protect an existing magnet with failing quench heaters without the need of expensive and time-consuming repair work.

Lastly, a further configuration is presented in Fig. 11, based on an alternative CLIQ design which is the subject of the following chapter.

5. CLIQ using a mutually-coupled external coil

An alternative quench protection system is presented based on a capacitive discharge through an external coil surrounding the solenoid magnet. Due to the strong coupling between the magnet and the external coil, the oscillation of the current in the external coil generates a magnetic-field change in the whole solenoid and thus introduces coupling losses in its coil.

Fig. 12 shows the measured discharged current I_C after triggering an 8.8 mF, 75 V CLIQ system through the normal-conducting bandage coil wrapped around the magnet. The number of turns of this bandage coil is about a fifth of that of the solenoid coil. As a result of the strong coupling between the solenoid and the external coil, the current in the solenoid oscillates at the same frequency. The coupling losses generated in the coil by effect of the introduced magnetic-field change are sufficient to initiate a quench in a large portion of the coil, as it can be observed in Fig. 12.

Used in this configuration, the CLIQ generates more coupling losses in the outer layers of the solenoid which are more closely coupled with the external coil and thus experience a faster change of the magnetic field. This result can be observed in Fig. 11, where it is shown that layer L10 is the first to quench, and the heat then orderly propagates to the inner layers. Furthermore, Fig. 13 shows the calculated effective resistance of each layer.

For a given capacitance and charging voltage, this alternative protection method typically introduces less loss in a solenoid than a standard CLIQ discharge if the external coil has less turns than the solenoid itself. As an example, Fig. 14 shows a comparison between the quench performance at $I_0 = 200$ A of a standard CLIQ

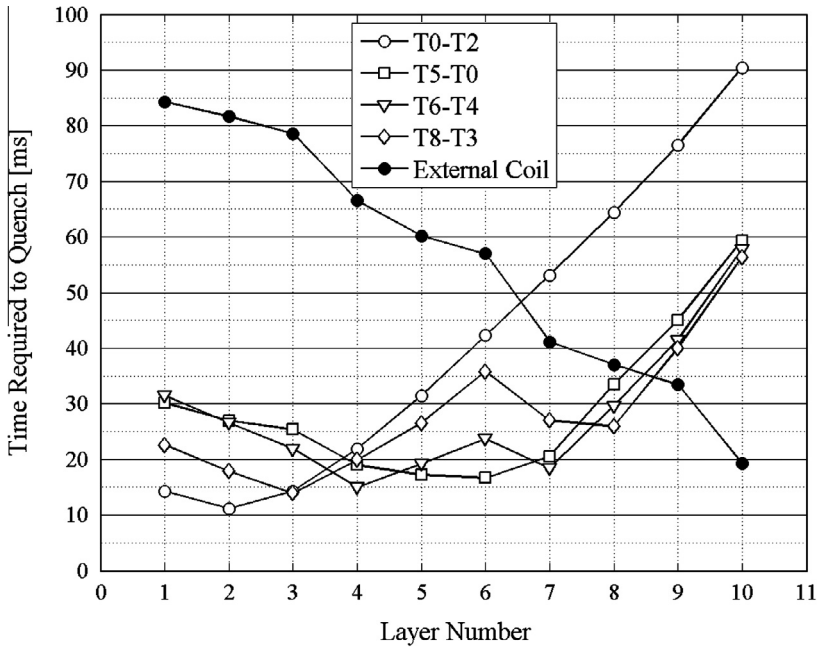

Fig. 11. Calculated time required to quench 90% of each of the ten layers of the solenoid magnet after a CLIQ discharge for various configurations ($I_0 = 300$ A, $U_0 = 75$ V, and $C = 8.8$ mF).

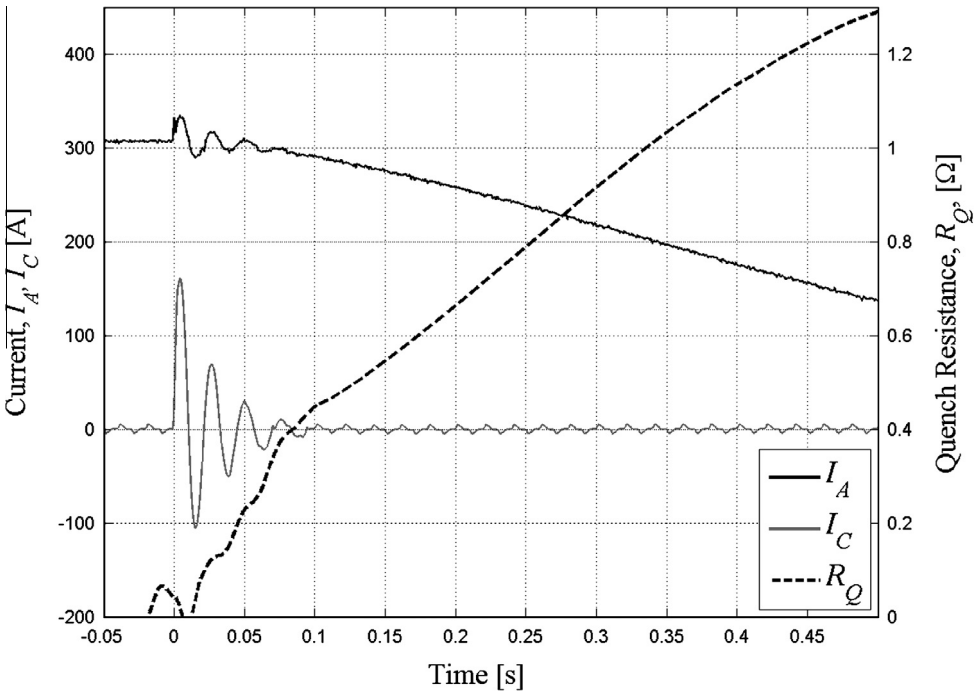

Fig. 12. Measured current I_A and I_C and calculated effective coil resistance R_Q, versus time after a CLIQ discharge through an external coil (I_0 = 300 A, U_0 = 75 V, and C = 8.8 mF).

(Configuration T6–T0) and a CLIQ using an external coil. One can observe that an 8.8 mF CLIQ using the external coil requires 20–30 ms more to quench the solenoid coil than a 4.7 mF standard CLIQ.

The new presented setup, despite its reduced efficiency with respect to a standard CLIQ, has a twofold advantage. Firstly, it is electrically insulated from the coil, and since it does not rely on thermal diffusion for the quench process the thickness of the insulation between the solenoid wire and the external coil can be increased without significant reduction of the quench performance. Secondly, the AC current is not injected directly in the coil, and thus the induced change in the coil transport current is limited. As a result, after triggering the CLIQ the coil current is not increased much with respect to its initial value and the Ohmic loss in the coil is not greatly enhanced. On the contrary, the additional Ohmic loss during the first CLIQ oscillations may be a significant setback when triggering a standard CLIQ system. As a result of this dual advantage, the maximum operating voltage and current of a CLIQ system using an external coil can be increased with less impact on the safety of the system.

The presented performance is achieved using a resistive bandage coil designed for mechanical reinforcement, hence not optimized for a CLIQ discharge. In general an even faster transition to normal state of the magnet coil can be expected in the case the CLIQ external coil is included in the design of the quench protection system from the start. A first obvious improvement would

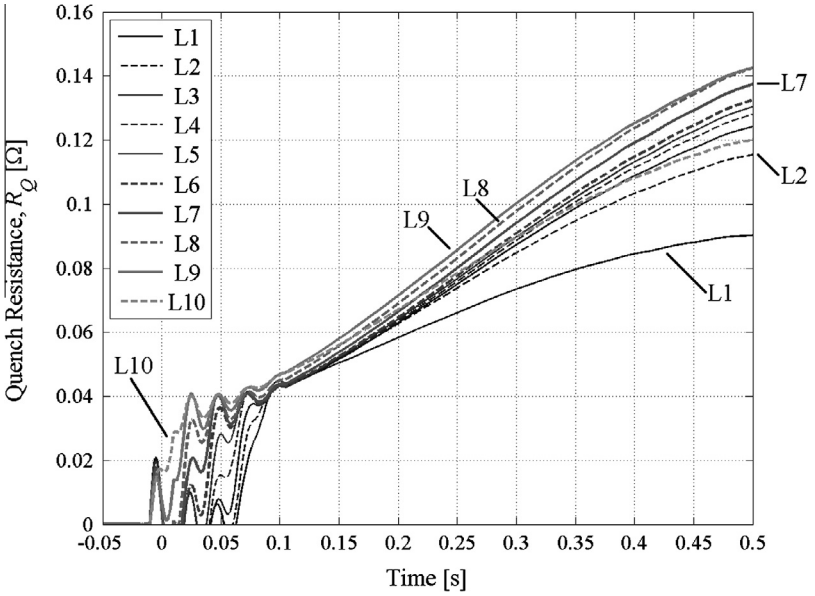

Fig. 13. Calculated effective quench resistance in each layer R_l versus time after a CLIQ discharge through an external coil (I_0 = 300 A, U_0 = 75 V, and C = 8.8 mF).

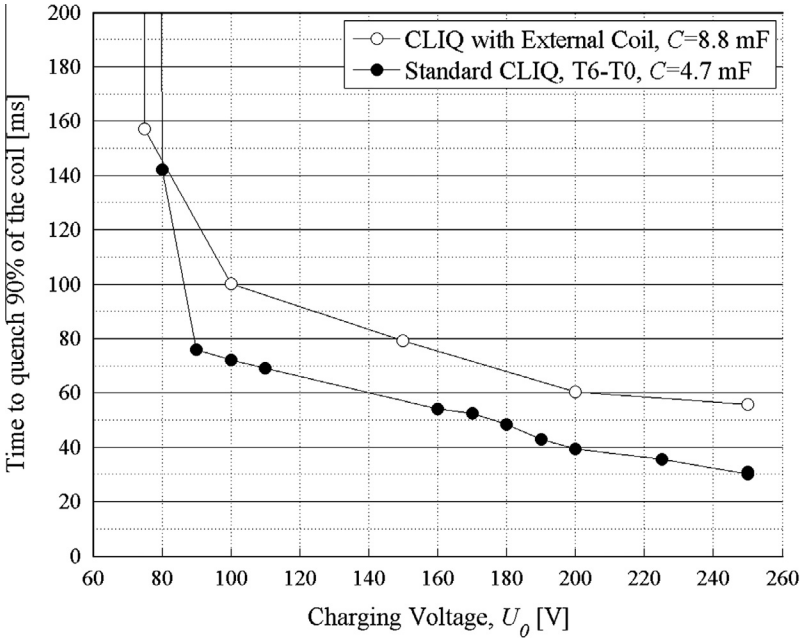

Fig. 14. Calculated time required to quench 90% of the coil versus U_0, after a standard CLIQ discharge (Configuration T6–T0, $C = 4.7$ mF) or a CLIQ discharge through an external coil ($C = 8.8$ mF) at $I_0 = 200$ A.

be the increase of the insulation layer between the external coil and the magnet, thus allowing a larger CLIQ charging voltage without dramatically increasing the risk of electrical breakdown.

An existing solenoid magnet can be protected with this method with relatively limited effort, provided a suitable coil mutually coupled with the solenoid coil is already present.

6. Conclusion

A new Coupling-Loss Induced Quench (CLIQ) protection system, recently developed at CERN, is thoroughly tested on a Nb–Ti solenoid magnet in order to assess its performance, highlight key operating parameters, and study new electrical configurations.

The CLIQ can introduce high coupling losses in the copper matrix of a superconductor by injecting an oscillating current through a current lead connected to an internal point of a magnet, and thus provoke a quench in the coil winding pack.

This system introduces similar losses at any current level because it relies on a capacitive discharge whose dynamics is not depending on the initial transport current in the coil. The deposited losses are proportional to the square of the CLIQ charging voltage, which is usually limited due to safety reason. For a given coil, an optimum choice of filament twist-pitch and of CLIQ capacitance exists that maximize the energy deposited in the magnet by a CLIQ discharge. The choice of the injection and extraction points is very important for the overall system performance. Connecting the CLIQ between an external current lead and the center of a solenoid magnet initiates the quench in the middle of the coil, thus accelerating the quench propagation. Alternatively, distributing two injection/extraction points in optimum positions can further enhance the system performance by simultaneously provoking a quench in two separate regions on the coil.

Finally, a new CLIQ electrical design is presented featuring a capacitive discharge through an external bandage coil surrounding the solenoid magnet. The fast change in the current in the external coil perturbs the magnetic field in the magnet and generates coupling losses. The maximum heat deposition occurs in the outer layers which are more closely coupled with the external coil. Whilst for a given charging voltage the quench performance of this configuration is not as good as that of a standard CLIQ system, the electrical insulation from the magnet constitutes an important advantage. In fact, the voltage and current of the discharge circuit are not directly affecting the solenoid coil, and thus higher safety limits can be accepted for their maximum allowed value.

Acknowledgements

The authors thank Nikolay Kopeykin and Igor Titenkov for the assembly of the test setup and Johan Bremer, Laetitia Dufay-Chanat, and Tiemo Winkler for their help to perform the CLIQ test campaigns at the CERN Cryogenic Laboratory.

References

[1] Ravaioli E et al. New, coupling loss induced, quench protection system for superconducting accelerator magnets. IEEE Trans Appl Supercond, vol. 24. [submitted for publication]
[2] Ravaioli E et al. A new hybrid protection system for high field superconducting magnets. EUCAS 2103, accepted for publication on SuST.
[3] Taylor JA et al. Quench protection for a 2-MJ magnet. Magn, IEEE Trans 1979;15(1):855–9.
[4] Schöttler RM, Lorenzen HW. Temperature and pressure rise in supercritical helium during the quench of indirectly cooled SC coils. Cryog Eng Conf Publ 1996;41:325–34.
[5] AC-current induced quench protection system. Application has been filed with the European Patent Office on June 28, 2013 under the application number EP13174323.9.
[6] SOLENO. A high-precision magnetic field, inductances and forces calculation code for air-core systems of multi-solenoids developed by the applied superconductivity applications group at the University of Twente, Enschede, the Netherlands.
[7] Verweij A. Electrodynamics of superconducting cables in accelerator magnets. PhD thesis University of Twente, The Netherlands, 1995. [chapter 4]
[8] Dudarev AV et al. Construction and test of the magnets for the AEgIS experiment. IEEE Trans Appl Supercond 2012;22(3):4500304.
[9] Dudarev AV et al. New fast response thin film based superconducting quench detectors. IEEE Trans Appl Supercond, vol. 24. [submitted for publication]